



# Self-assembled nanoparticles based on amphiphilic chitosan derivative and hyaluronic acid for gene delivery

Ya Liu, Ming Kong, Xiao Jie Cheng, Qian Qian Wang, Li Ming Jiang, Xi Guang Chen\*

College of Marine Life Science, Ocean University of China, Qingdao, 266003, PR China

## ARTICLE INFO

### Article history:

Received 13 September 2012

Received in revised form

18 December 2012

Accepted 21 December 2012

Available online 5 January 2013

### Keywords:

OCMCS

HA

DNA

NPs

Gene vector

## ABSTRACT

The present work described nanoparticles (NPs) made of oleoyl-carboxymethyl-chitosan (OCMCS)/hyaluronic acid (HA) using coacervation process as novel potential carriers for gene delivery. An N/P ratio of 5 and OCMCS/HA weight ratio of 4 were the optimal conditions leading to the smallest (164.94 nm), positive charged (+14.2 mV) and monodispersed NPs. OCMCS-HA/DNA (OHD) NPs showed higher in vitro DNA release rates and increased cellular uptake by Caco-2 cells due to the HA involved in NPs. The MTT survival assay indicated no significant cytotoxicity. The transfection efficiency of OHD NPs was 5-fold higher than OCMCS/DNA (OD) NPs; however, it decreased significantly in the presence of excess free HA. The results indicated that OHD NPs internalized in Caco-2 cells were mediated by the hyaluronan receptor CD44. The data obtained in the present research gave evidence of the potential of OHD NPs for the targeting and further transfer of genes to the epithelial cells.

© 2012 Elsevier Ltd. All rights reserved.

## 1. Introduction

Gene delivery is a promising strategy as the encoded protein can be expressed in the host in its natural form (without denaturation or modification), and caused prolonged expression of the protein (Mao, Sun, & Kissel, 2010). The gastrointestinal (GI) system is an excellent target for noninvasive localized drug delivery due to its large surface area and its accessibility. For this reason, the GI tract has been considered as an attractive target for gene therapy interventions (Nandedkar, 2009). The success in gene therapeutic strategies depends on an efficient system for the delivery of nucleic acid into the target cells (Vadolas, Williamson, & Ioannou, 2002). In recent years, non-viral vectors and especially those resulting from the use of nanotechnologies have received increasing attention for achieving the delivery of genetic material to the GI tract (Luten, van Nostrum, De Smedt, & Hennink, 2008).

Cationic polymers have been shown as promising carriers among the non-viral gene delivery systems. Many cationic polymers, such as chitosan, polylysine, polyethyleneimine, dendrimers, poly (α-(4-aminobutyl)-L-glycolic acid) as well as cationic liposomes have been investigated for gene delivery (Mohammadi et al., 2011). Chitosan has been investigated as nonviral vector for gene

delivery because of its ability to condense gene into nanoparticles that are appropriate to be endocytosed by cells, and subsequently be released from endosomes and enter nucleus (Muzzarelli, 2010a). Furthermore, chitosan is an ideal candidate for oral DNA delivery due to its good biocompatibility and high positive charge density conferring it mucoadhesive properties (Lai, Wang, & Hanes, 2009; Muzzarelli, 2010b).

However, chitosan shows two major disadvantages: one is poor solubility because the amino groups on chitosan are only partially protonized at physiological pH 7.4. The other is low transfection efficiency (Gao et al., 2008). In our previous research, oleoyl-carboxymethyl-chitosan (OCMCS) has been synthesized and proposed as one of water-soluble chitosan derivatives over a wide pH range (Liu, Cheng, et al., 2012; Liu, Zang, et al., 2012). The transfection efficiency of chitosan vectors can be improved by combining chitosan with cationic or anionic biopolymers, such as polyethyleneimine (Zhao et al., 2009) or arginine (Gao et al., 2008), prior to the addition of DNA. The choice of biopolymer greatly influences the specificity, stability, and size of the assembled nanoparticles (Duceppe & Tabrizian, 2009). Hyaluronic acid (HA) is another biocompatible anionic biopolymer naturally found in humans and is used for a great number of clinical applications (Muzzarelli, Greco, Busilacchi, Sollazzo, & Gigante, 2012). This biopolymer has some advantageous properties, including its ability to bind various cellular receptors such as CD44 (Aruffo, Stamenkovic, Melnick, Underhill, & Seed, 1990), which is expressed in normal human epithelium cells, chondrocytes and cancerous cells (Marhaba & Zoller, 2004). The targeting of the gene carriers

\* Corresponding author at: College of Marine Life Science, Ocean University of China, 5# Yushan Road, Qingdao 266003, China. Tel.: +86 0532 82032586; fax: +86 0532 82032586.

E-mail addresses: [xgchen@ouc.edu.cn](mailto:xgchen@ouc.edu.cn), [qqsn160@163.com](mailto:qqsn160@163.com) (X.G. Chen).

is of particular interest for oral therapy (Merdan, Kopecek, & Kissel, 2002), as this would increase the efficiency (Li & Huang, 2006) and reduce side effects compared to non-targeted treatments such as death of healthy tissues.

Our goal in the present work was to evaluate the potential of a novel gene nanocarrier, consisting of OCMCS and HA, specially designed for the specific targeting and intracellular delivery of genes into the intestinal epithelial cells.

## 2. Materials and methods

### 2.1. Materials

Chitosan (Mw = 50 kDa, degree of deacetylation = 93.15%) was made from crab shell and obtained from Laizhou Haili Biological Product Co., Ltd. (Shandong China). Hyaluronic acid, with a molecular weight of 5 kDa, was purchased from C.P. Freda Pharmaceutical Co. Ltd. (Shangdong, China).

Caco-2 cells were obtained from the American Type Culture Collection (Rockville, MD, USA) and cultured in Dulbecco's Modified Eagle Medium (DMEM) (Gibco, Grand Island, NY, USA) containing 10% fetal calf serum. 3-(4, 5-Dimethylthiazol-2-yl)-2, 5-diphenyl-tetrazolium bromide (MTT) was obtained from Amresco (Solon, OH).

Lipofectamine™ 2000 was obtained from Invitrogen (USA). Plasmids (pEGFP-N2, 4.7 kb) containing a CMV promoter and an enhanced green fluorescence protein reporter were obtained from BD Biosciences Clontech (Palo Alto, CA, USA). pEGFP-N2 was amplified and isolated using a Plasmid Mega Kit (QIAGEN, Valencia, CA, USA). The recovered plasmids were stored at 4 °C in sterile deionized (DI) water. The purity of plasmids was analyzed by gel electrophoresis (0.8% agarose), while their concentration was measured by UV absorption at 260 nm (V-530, Jasco, Tokyo, Japan).

### 2.2. Preparation of OCMCS/DNA (OD) NPs and OCMCS-HA/DNA (OHD) NPs

Oleoyl-carboxymethyl-chitosan (OCMCS) was synthesized by reaction of chitosan with chloroacetic acid and oleoyl chloride as described in our previous study (Li et al., 2006). Solutions of OCMCS at different concentrations were prepared in phosphate buffer saline (PBS, pH 6.5) in order to achieve N/P ratios of 0.5, 1, 2, 5, 10, 15, and 20 (an amino group to a phosphate group ratio hereafter was defined as charge or N/P ratio). A DNA solution of 50 µg/ml in 25 mM of sodium sulfate was prepared. An equal volume of chitosan solution (from each concentration) and DNA solution were added (by dropping slowly) together while stirred at various speed (100–2000 rpm). The final volume of the mixture in each preparation was limited to below 500 µl in order to yield uniform NPs.

OHD NPs were prepared according to the method described by Duceppe and Tabrizian (2009). In brief, 10 mg HA was dissolved in 4 ml of distilled water under magnetic stirring. The OCMCS solution was stirred at a rate of 3000 rpm for 30 min, mixed into the HA solution and stirred for 10 min. Seven different mixtures were prepared with CS:HA weight ratios at 1:1, 2:1, 3:1, 4:1, 5:1, 6:1, and 7:1. The required volume of 50 µg/ml plasmid DNA was gently added to OCMCS/HA solution to form complexes of a selected N/P ratio. The mixture was vortexed rapidly for 3–5 s and left for 1 h at room temperature for the complexes to completely form.

### 2.3. Particle size, zeta potential and surface morphology

The Z-average hydrodynamic diameter and surface charge of NPs were determined by dynamic light scattering (DLS) using Zetasizer Nano ZS (Malvern Instruments Ltd., UK) at room temperature. The NPs were prepared and analyzed in 1 ml distilled water at

25 °C. All samples were measured in triplicate. The morphological characterizations of the NPs were viewed using scanning electron microscopy (SEM, JSM-330A, Japan) and atomic force microscopy (AFM, Dualscope C26, DME, Denmark).

### 2.4. Gel retarding analysis

OHD NPs were evaluated by agarose gel electrophoresis. The NPs and the naked plasmid were loaded onto a 1% agarose gel containing ethidium bromide in Tris–borate EDTA buffer at pH 8.0. The samples were run on the gel at 120 V for 30 min. The gel was then photographed using a GDS-8000 (UVP, USA).

OHD NPs (N/P ratio 5) prepared with OCMCS: HA weight ratios of 4:1 and naked DNA solution (each containing 1 µg of DNA) were added to 10 U of *NotI* and 15 U *HindIII* (Sigma–Aldrich, USA) and kept in a water bath for 30 min at 37 °C. In addition, different concentrations (56–336 ng/µl) of chitosanase (from streptomyces species, activity 18 units/mg, Sigma–Aldrich, USA) were added and the NP–chitosanase solution was maintained in a water bath for 4 h at 37 °C. Agarose gel (1%) electrophoresis was repeated, as described above.

### 2.5. Stability of OHD NPs

OHD NPs suspension (1 mg/ml, 1 ml) was placed into a cellulose membrane dialysis tube (molecular weight cutoff 8000–10,000). The tube was introduced into the different kinds of simulated fluid referred to Mohammad Reza (Saboktakin, Tabatabaie, Maharramov, & Ramazanov, 2011) and kept in a water bath at 37 °C. At predetermined time intervals (between 0 h and 6 h), whole medium was removed and replaced by fresh simulated fluid. The protocol of using the simulated fluids at different pH was as follows:

- 0–2 h: simulated gastric fluid, pH 1.2
- 2–4 h: simulated duodenum fluid, pH 6.0
- 4–6 h: simulated intercellular spaces of enterocytes fluid, pH 7.4

Simulated gastric fluid (SGF, pH 1.2) consisted of NaCl (0.2 g), HCl (7 ml) and pepsin (3.2 g); pH was adjusted by NaOH to  $1.2 \pm 0.5$ . Simulated intestinal fluid (SIF) consisted of  $\text{KH}_2\text{PO}_4$  (6.8 g), 0.2 N NaOH (190 ml), and pancreatin (10.0 g). SIF was adjusted by NaOH to  $7.4 \pm 0.1$  to obtain simulated intercellular spaces of enterocytes fluid (SISEF). Simulated duodenum fluid (SDF) pH 6.0 was prepared by mixing SGF pH 1.2 and SISEF pH 7.4 in a ratio of 30:70. At predetermined time intervals (0 h, 2 h, 4 h and 6 h), the particle size was evaluated via a Zetasizer (Malvern Instruments, UK) and the morphology of the OHD NPs was observed by transmission electron microscope (100 CX II, Japan).

### 2.6. Evaluation of DNA loading and release

The OD NPs and OHD NPs (N/P ratio 5 and OCMCS/HA weight ratio 4) were formed according to the method described in Section 2.2. After complex was completely formed at ambient temperature for 30 min, the turbid solution was centrifuged at  $20,000 \times g$  at 4 °C for 30 min and the supernatant was collected to determine the amount of free DNA. The loading efficiency (LE %) of DNA was calculated by Eq. (1), and the analyses were performed in triplicates.

$$\text{LE\% of DNA} = \left[ \frac{A - B}{A} \right] \times 100\% \quad (1)$$

where  $A$  is the total concentration of DNA (mg/ml) and  $B$  is the concentration of unloaded DNA (mg/ml).

Phosphate buffer saline (PBS, pH 7.4) was used as media for the DNA release study. Dried OD NPs and OHD NPs (3.9 mg) and buffer solution (1.2 ml) were placed in a micro tube and incubated in a

water bath at  $37 \pm 0.5^\circ\text{C}$ , respectively. At the sampling time, the incubated dispersing solution was centrifuged, and 400  $\mu\text{l}$  of supernatant was collected for evaluation of the amount of released DNA using a spectrophotometer at 258 nm. An equal volume of fresh buffer was, then, replaced in the solution and the same procedure was repeated for the next sampling time. The accumulative release percentage ( $Q\%$ ) was calculated by Eq. (2), and the analyses were performed in triplicates.

$$Q\% = \frac{C_n \cdot V + V_i \sum_{i=0}^{n-1} C_i}{\text{DNA}_t \times \text{LE}\%} \times 100 \quad (2)$$

where  $C_n$  is the DNA concentration at  $T_n$ ,  $V$  is the total volume of release medium,  $V_i$  is the sampling volume at  $T_i$ ,  $C_i$  is the DNA concentration at  $T_i$  (both  $V_0$  and  $C_0$  were equal to zero),  $\text{DNA}_t$  is the total amount of DNA used for preparation of the original mixture,  $\text{LE}\%$  is the loading efficiency of DNA loaded into the nanoparticulate systems.

## 2.7. Cytotoxicity assays

The cell viability was determined using the MTT method. Caco-2 cells were seeded at a density of  $5 \times 10^4$  cells per well in 100  $\mu\text{l}$  of culture medium in 96-well plates and grown overnight. Immediately after culture medium was removed, either OD NPs or OHD NPs (N/P ratio 5, OCMCS: HA weight ratios 4:1), at OCMCS concentrations ranging from 20  $\mu\text{g}/\text{ml}$  to 200  $\mu\text{g}/\text{ml}$ , suspended in fresh serum free media, were applied to the cells. In another group of cells, culture media was replaced by fresh serum free media containing Lipofectamine<sup>TM</sup> 2000/DNA (20  $\mu\text{g}/\text{ml}$ ). A group of cells treated with only fresh culture medium were used as controls.

The percentage of viability was expressed as relative growth rate (RGR %) by Eq. (3): Tests were performed in quadruplicate for each sample.

$$\text{RGR}\% = \frac{D_t}{D_{nc}} \times 100\% \quad (3)$$

where  $D_t$  and  $D_{nc}$  were the absorbance of the tested sample and the negative control.

## 2.8. Cellular uptake study

In order to know the cellular uptake of the OD NPs and OHD NPs, OCMCS was fluorescently labeled with FITC. FITC-labeled OCMCS (FITC-OCMCS) was synthesized by the reaction between the isothiocyanate group of FITC and the primary amino group of OCMCS (Wan, Hu, & Yuan, 2004). NPs were prepared at N/P ratio 5 for OCMCS: HA weight ratios 4:1. Caco-2 cells were seeded in a 24-well plate at a density of  $1 \times 10^5$  cells per well in 500  $\mu\text{l}$  growth medium and allowed to attach for 24 h. Then the culture medium was replaced by transport buffer (phosphate-buffered saline, PBS, pH 7.4) and preincubated at  $37^\circ\text{C}$  for 30 min. After equilibration, the culture medium was changed with 100  $\mu\text{l}$  of freshly prepared FITC labeled NP suspension (100  $\mu\text{g}/\text{ml}$  in PBS) and incubated at  $37^\circ\text{C}$  for 4 h. To investigate influence of the extra HA on cellular uptake of NPs, free HA at concentrations 10 times greater than the HA content of the NPs was added to the cells and incubated for 20 min at  $37^\circ\text{C}$ . To measure the fluorescence intensity of the cells, cells after treated with NPs were carefully washed three times with PBS, then trypsinized and resuspended in the medium. Then cells were centrifuged and washed three times with PBS. The cell resuspension was finally subjected to FACSCalibur (Becton Dickinson, USA) and analyzed with CellQuest software through fluorescence channel 1 (FL1).

## 2.9. In vitro transfection experiment

Caco-2 cells were seeded into 24-well plates at a density of  $1 \times 10^5$  cells per well in 500  $\mu\text{l}$  of culture medium and incubated for 24 h prior to transfection. Then, the media was replaced with fresh growth medium without antibiotics containing naked DNA or OD NPs (negative controls) with N/P ratio of 5 or OHD NPs (with N/P ratio of 5 and OCMCS: HA weight ratio of 4:1) (test groups) or Lipofectamine<sup>TM</sup> 2000 (positive controls) with DNA concentration 2.5  $\mu\text{g}/\text{well}$ . Media were replaced by fresh culture medium after 8 h and cells were incubated for an additional 48 h. All transfection experiments were performed in triplicate. EGFP-positive transfected cells were detected using fluorescence microscope (Nikon-TE2000-U, Japan). Finally, cells were collected and resuspended in PBS (pH 7.4). The transfection results were measured using a FACSCalibur through fluorescence channel 1 (FL1).

An additional transfection study was performed to investigate the potential utilization of CD44 in aiding transportation of pEGFP into the cell by blocking the receptor with an excess of HA. Free HA (at concentrations 10 times greater than the HA content of the NPs) was added to the cells and incubated for 20 min at  $37^\circ\text{C}$ . After incubation, polysaccharide solutions were aspirated, and NPs containing DNA in solution were introduced to the cells and incubated for 8 h at  $37^\circ\text{C}$ , as described above. The transfection efficiency was determined by fluorescent microscopy and FACS, as mentioned above.

## 2.10. Statistical analysis

The statistical significance was studied by one-way ANOVA and the  $t$ -test. Differences were considered to be significant at a level of  $p < 0.05$ .

# 3. Results and discussion

## 3.1. Physicochemical characterization of OHD NPs

The OHD NPs were formed as a result of complex coacervation. The particle size and surface charge of gene delivery systems was known to be the major factors influencing their transfection efficiency (Romoren, Pedersen, Smistad, Evensen, & Thu, 2003). The size of nanoparticles is important for cellular uptake and can be affected by the N/P ratio and OCMCS: HA weight ratio during the formation of coacervates as demonstrated in Fig. 1A.

The effect of charge ratio on the particle size and surface charge was examined at N/P ratios of 0.5–20. As shown in Fig. 1A(a), OHD NPs with N/P ratios of 5 had the smallest sizes. The zeta potential of OHD NPs increased slightly with the N/P ratio (ranging from  $-3.42$  to  $+15.87$  mV). At N/P ratio below 1, the concentration of OCMCS was lower than the concentration of plasmid and was unable to condense DNA which resulted in negative zeta potential. The increase of surface charge with N/P ratio over 1 could be result from the exclusion of redundant positive charge provided by OCMCS inside NPs.

The influence of the OCMCS/HA ratio (w/w) on the size of nanoparticles was shown in Fig. 1A(b). The size and zeta potential of the nanoparticles were dependent on the composition, with an increase in size and a decrease in the surface charge with increasing HA content. The NPs showed the smallest particle size (164.94 nm) with OCMCS/HA weight ratio of 4. At OCMCS/HA weight ratio below 4, significant decreases turned up in particle sizes with increasing ratios, however, it only varied slightly with N/P ratio over 4. The zeta potential becomes more positive as the amount of OCMCS within the polyelectrolyte complex increases (from  $+7.51$  to  $+16.46$  mV).

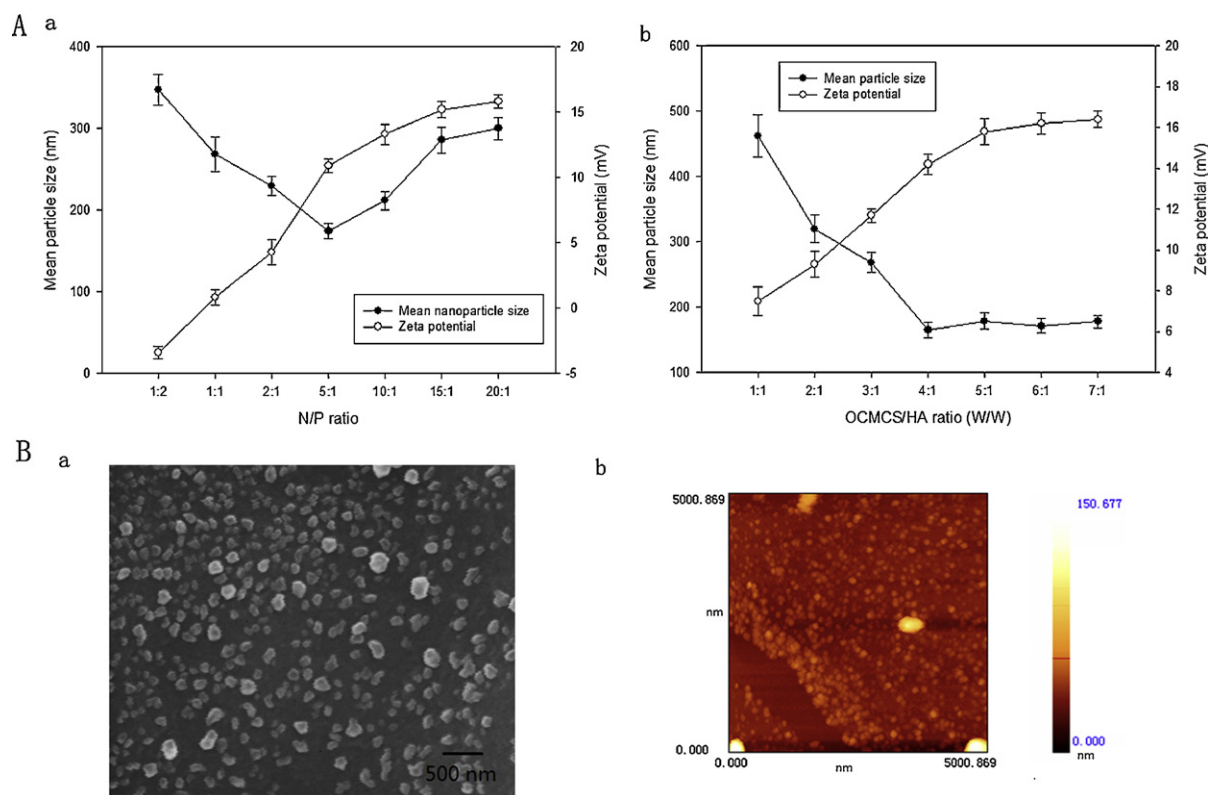


**Fig. 1.** A, effect of N/P ratio (a) and OCMCS/HA ratio (w/w) (b) on particle size and zeta potential of OCMCS-HA/DNA NPs; B, physical characterization of OCMCS-HA/DNA NPs (N/P = 5, OCMCS/HA = 4) by SEM (a) and AFM (b) imaging.

The surface charge should be considered when the complex is introduced into the body. Although positively charged nanoparticles can attach to the cell membrane, which is negatively charged, and enter the cell more easily (Mansouria et al., 2006), NPs with high positive charge should be avoided because it might cause toxic side effects for cells, nonspecific interactions between complex and cells, and also exchange reactions of DNA with negatively charged macromolecules existing in the body during delivery (Schatzlein, 2001). These experimental conditions were maintained for further analyses, because the OHD NPs with N/P ratio 5 and OCMCS/HA ratio (w/w) 4 presented the desired features in terms of size and zeta potential.

The morphological characterizations of the OHD NPs (N/P = 5, OCMCS/HA = 4) were evaluated by SEM (Fig. 1B(a)) and TEM (Fig. 1B(b)). The nanoparticles had similar nanometric dimension and showed round shaped particles with a size around 150 nm, which was in agreement with the diameter obtained by DLS.

### 3.2. Integrity and protection against nuclease degradation of the associated DNA

Integrity of the associated plasmid DNA and protection against nuclease degradation by nanoparticles were determined by agarose gel electrophoresis. Gel electrophoresis indicated when the N/P ratio was above 1, the DNA was totally retained within the gel loading well, which illustrated the complete coalesce of plasmid with OCMCS (Fig. 2A).

As revealed in Fig. 2B, NPs with OCMCS-HA protected DNA from degradation by *NotI* and *HindIII* (lane 5) while naked DNA was completely degraded (lanes 2 and 3). The integrity of the associated DNA was confirmed after degradation of the NPs with chitosanase (lane 4). The NPs with OCMCS-HA (lane 7) protected the DNA against degradation when chitosanase was added following *NotI*

and *HindIII*. On the contrary, DNA was completely degraded (lane 6) when chitosanase was added previously. The results indicated that OCMCS-HA was capable to loaded DNA efficiently and preserve its integrity.

### 3.3. Stability of OHD NPs

The physical stability of OHD NPs was evaluated by measuring the sizes of the nanoparticles at pH 1.2, 6.0 and 7.4, simulating the environments of stomach, intestine and the body fluid at the intercellular spaces of enterocytes, respectively (Table 1). No significant differences were detected in the sizes of OHD NPs at pH 1.2 in SGF and pH 6.0 in SDF, while the size slightly increased after incubated at pH 7.4 in SISEF.

The corresponding TEM images of OHD NPs at 0 h, 2 h, 4 h and 6 h were used to visualize morphology of OHD NPs at different medium (Fig. 3A). It was known that the  $pK_a$  value of the amino groups ( $-NH_4^+$ ) on OCMCS was about 6.5 (Hu et al., 2002) and OCMCS also had carboxylate groups ( $-COO^-$ ) ( $pK_a$  2.0–4.0) on its backbone as well as HA (Casu & Gennaro, 1975). Additionally there were many phosphate groups ( $PO_4^{3-}$ ) on DNA, whose  $pK_a$  value was 1.0–2.1. At pH 1.2 in SGF and pH 6.0 in SDF, the  $-NH_4^+$  on OCMCS were protonized,  $PO_4^{3-}$  on DNA were ionized, and  $-COO^-$  on HA were partially or completely disassociated. Therefore, positively charged

**Table 1**  
Size of OCMCS-HA/DNA NPs in different pH medium.

OCMCS-HA/DNA NPs	Particle size (nm)
Untreated	157.41 ± 26.82
pH 1.2	148.41 ± 19.21
pH 6.0	151.41 ± 22.12
pH 7.4	187.41 ± 20.57

Each value represents the mean ± S.D. (n = 3).



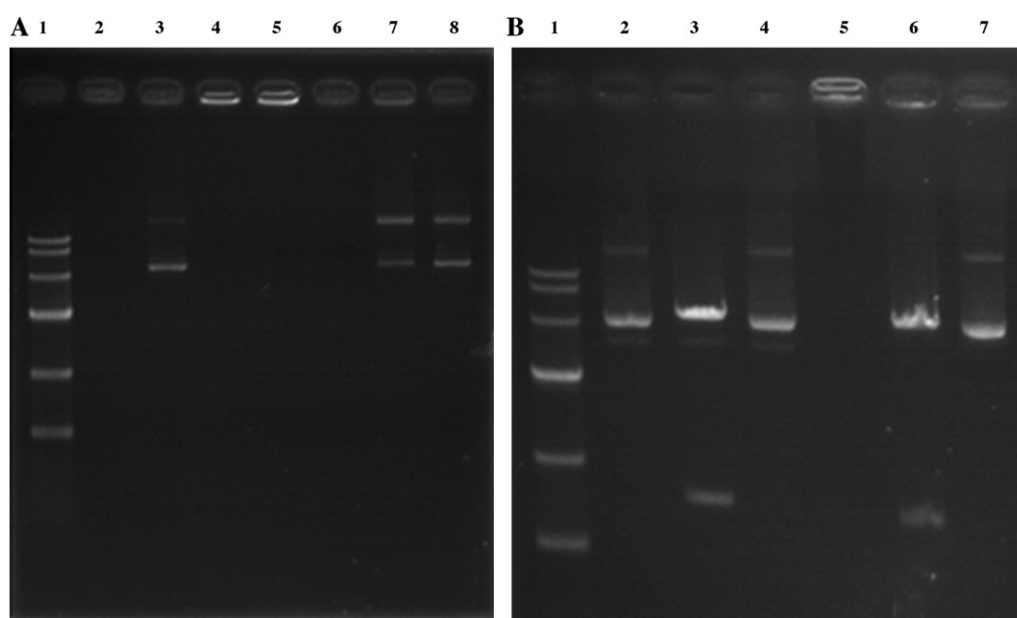


**Fig. 2.** Gel retardation analysis of OCMCS-HA/DNA nanoparticles (A); Lane 1, DNA ladder; Lane 2, OCMCS solution; Lane 3, naked DNA; Lanes 4–8, OCMCS-HA/DNA NPs prepared at N/P ratios of 10:1, 5:1, 1:1, 1:2 and 1:4, respectively. Electrophoresis of OCMCS-HA/DNA NPs to determine the integrity of plasmid (B); NPs were digested with chitosanase and DNase after synthesis. Lane 1, DNA ladder; Lane 2, naked DNA; Lane 3, naked DNA + NotI and HindIII; Lane 4, OCMCS-HA/DNA NPs + chitosanase; Lane 5, OCMCS-HA/DNA NPs + NotI and HindIII; Lane 6, OCMCS-HA/DNA NPs + chitosanase + NotI and HindIII; Lane 7, OCMCS-HA/DNA NPs + NotI and HindIII + chitosanase.

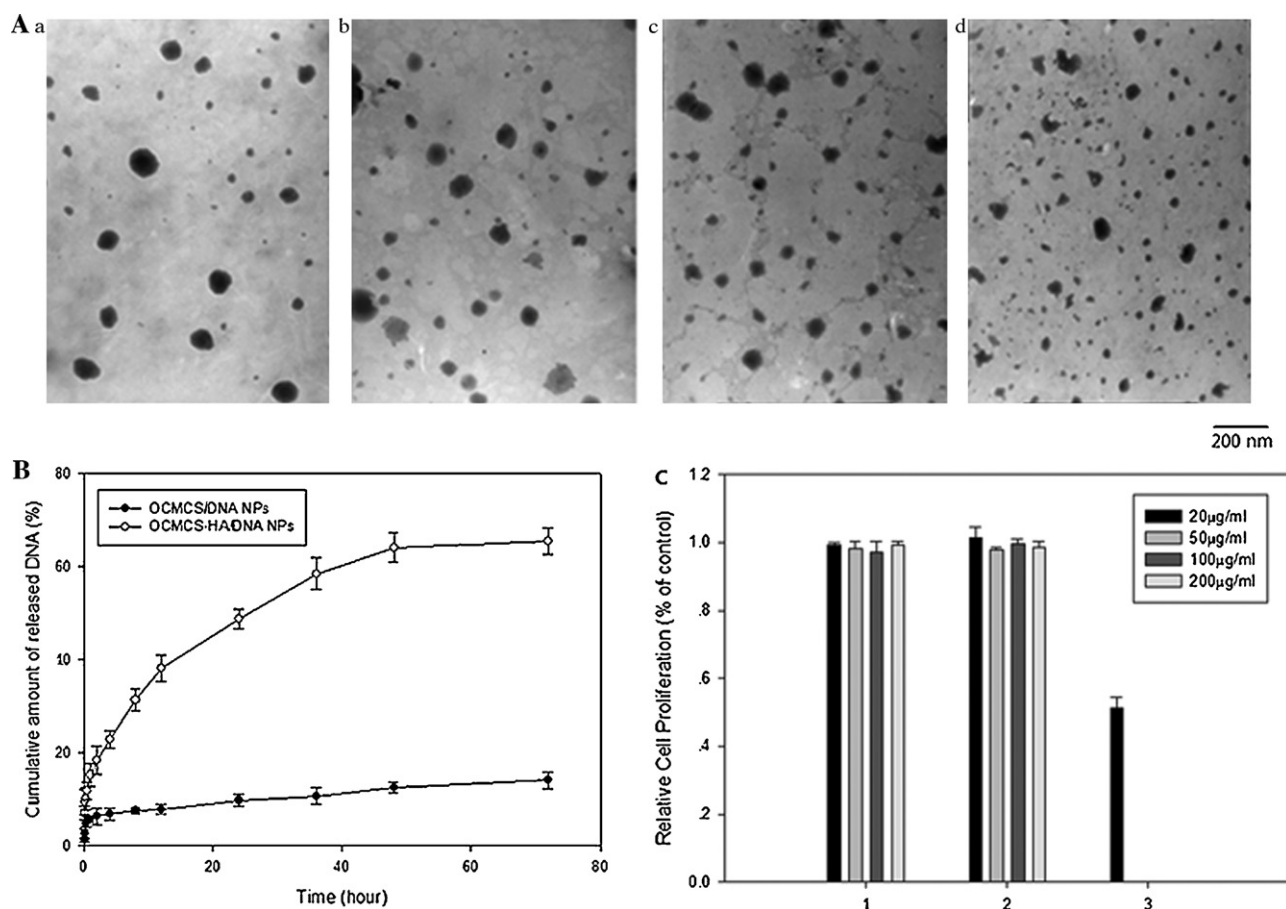


**Fig. 3.** A, TEM images of OCMCS-HA/NPs at 0 h (a), 2 h (b), 4 h (c) and 6 h (d) in different pH medium; 0–2 h: SGF, pH 1.2 2–4 h: SDF, pH 6.0, 4–6 h: SISEF, pH 7.4; B, in vitro releasing profile of DNA at  $37 \pm 5^\circ\text{C}$  from OCMCS-HA/DNA NPs in PBS (pH 7.4); C, % cell viability at various concentrations of OCMCS/DNA NPs (1), OCMCS-HA/DNA NPs (2) and Lipofectamine™ 2000/DNA (3).

**Table 2**

Loading efficiency (LE) and in vitro release amount of DNA in OCMCS/DNA NPs and OCMCS-HA/DNA NPs (N/P ratio 5 and OCMCS/HA weight ratio 4).

Samples	LE of DNA (%)	In vitro release amount of DNA (%)
OCMCS/DNA NPs	94.21 ± 5.62	14.12 ± 1.83
OCMCS-HA/DNA NPs	91.37 ± 3.81	65.57 ± 2.86

OCMCS and negative charged HA, DNA were able to form polyelectrolyte complexes via electrostatic interaction, resulting in particles with a spherical shape. At pH 7.4 in SISEF, partial  $\text{-NH}_4^+$  on OCMCS had partially become deprotonized and weakened the electrostatic interaction between OCMCS, HA and DNA; the structure of OHD NPs had gotten loosened. The results indicated OHD NPs had the ability to deliver DNA to small intestine and were more likely to release the loaded DNA only when they infiltrated into the intestinal mucosa and approach enterocytes.

### 3.4. DNA loading and release in vitro

The LE of DNA into the complex was calculated based on the total amount of DNA added in the NPs preparation step. As shown in Table 2, the LE of DNA in OD NPs and OHD NPs was  $94.21 \pm 5.62\%$  and  $91.37 \pm 3.81\%$ , respectively.

The releasing profiles of DNA from the OD NPs and OHD NPs were investigated in vitro at  $37 \pm 0.5^\circ\text{C}$  for 3 days in phosphate buffer saline (PBS, pH 7.4). The amount of released DNA was measured by a spectrophotometer at 258 nm. It should be pointed out that the OD NPs and OHD NPs incubated in all media gave quite different releasing profiles (Fig. 3B). The DNA loaded in OD NPs was released very slowly, with final release of approximately 14% within 72 h of incubation. The strong electrostatic interaction between OCMCS and DNA might result in the slow DNA release. Otherwise, the DNA loaded in OHD NPs was released in a faster, continuous manner, with a final release of approximately 65% in the same period.

For OHD NPs, the release of DNA was markedly divided into two stages based on the release rate. For the initial stage, the first 4 h, in the release rate was very fast (burst effect) (Mao et al., 2001). The mechanism of DNA release in this stage might be explained by the diffusion of DNA localized on the NPs surface. Because of the existence of negative charged HA, the electrostatic interaction between these oppositely charged macromolecules-OCMCS and DNA was weakened, which allowed better diffusion of DNA from the nanoparticles (Elfinger et al., 2009).

### 3.5. Cytotoxicity assays

In order to develop OHD NPs as novel gene delivery carriers for GI system, an assessment of any potential toxic interaction with intestinal epithelia is very important. In this study, the cytotoxicity of OD NPs and OHD NPs to Caco-2 cells was estimated using the MTT assay. As the NPs dose increased to  $200 \mu\text{g/ml}$ , both OD NPs and OHD NPs showed a slight increase in cellular toxicity (Fig. 3C). However, the average cell viability of OHD NPs was more than 90%, which was much higher than that of Lipofectamine™ 2000, and showed less than 60% viability. These cytotoxicity results indicate that OHD NPs should be a safer carrier than Lipofectamine™ 2000 and specify a safe range for the application of OHD NPs ( $20\text{--}200 \mu\text{g/ml}$ ) to Caco-2 cells.

### 3.6. Cellular uptake study

To estimate the amount of DNA internalized into cells and measure the fluorescent intensity, cells were subjected to FACSCalibur. Compared with OD NPs, about 2-fold higher mean fluorescence

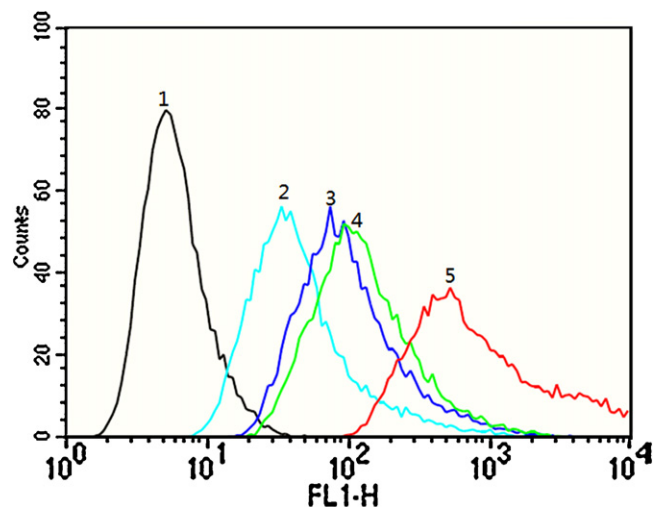


**Fig. 4.** The FCM pictures of control cells and cells treated with FITC labeled NPs of collected Caco-2 cells. Untreated cells were used as negative control. 1: Control, 2: free HA + OCMCS-HA/DNA NPs, 3: Free HA + OCMCS/DNA NPs, 4: OCMCS/DNA NPs, 5: OCMCS-HA/DNA NPs.

intensity ( $982.1 \pm 43.7$ ) was detected in Caco-2 cells treated with OHD NPs at the same tested concentration (Fig. 4). The result demonstrated that chitosan modified with HA could improve its cellular uptake. HA was known for its implication in several processes, such as the regeneration of corneal and conjunctival epithelial cells, through an interaction with the CD44 receptor (Schmitz et al., 2007). With the objective of elucidating whether CD44 is responsible for the receptor-mediated uptake, we blocked the receptor by the addition of excess free HA. As expected, the cellular uptake of the OHD NPs varied negligibly after the receptor blockage. On the contrary, the excess free HA only cause a slight decrease of mean fluorescence intensity when the cells were treated with OD NPs. Consequently, we concluded that OHD NPs were internalized by fluid endocytosis and that this endocytic process was mediated by the hyaluronan receptor.

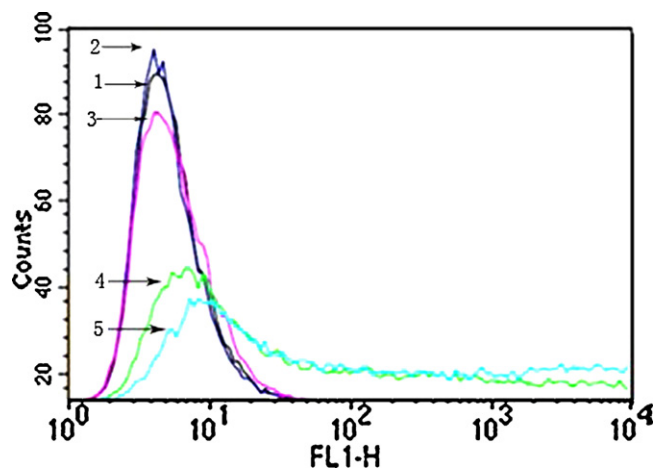


**Fig. 5.** The FCM pictures of Caco-2 cells transfected with OCMCS/DNA NPs and OCMCS-HA/DNA NPs. Untreated cells were used as negative control and cells transfected with Lipofectamine™ 2000/DNA were used as positive control. 1: Untreated cells, 2: naked DNA, 3: OCMCS/DNA NPs, 4: OCMCS-HA/DNA NPs, 5: Lipofectamine™ 2000/DNA.

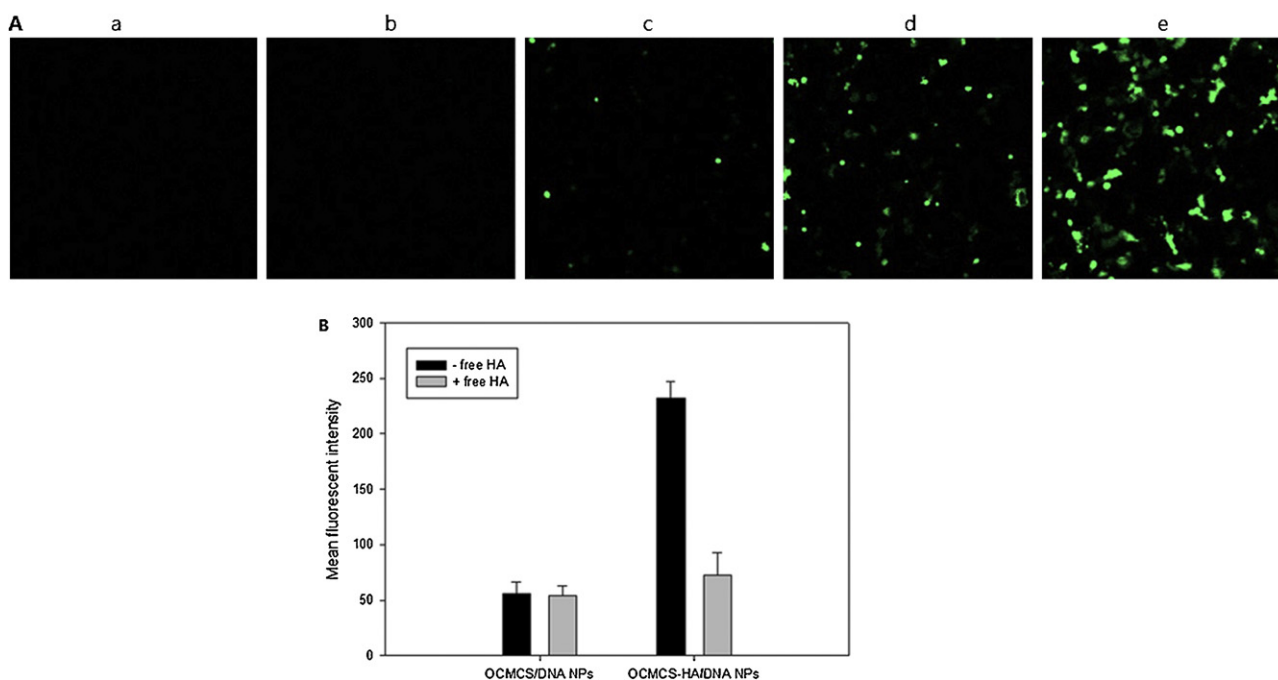


**Fig. 6.** A, Images of Caco-2 cells transfected with OCMCS/DNA NPs and OCMCS-HA/DNA NPs (N/P ratio = 5, OCMCS/HA weight ratio = 4) observed under fluorescent microscope (20 $\times$  magnification). Untreated cells were used as negative control and cells transfected with Lipofectamine<sup>TM</sup> 2000/DNA were used as positive control. Untreated cells (a), naked DNA (b), OCMCS/DNA NPs (c), OCMCS-HA/DNA NPs (d), Lipofectamine<sup>TM</sup> 2000/DNA (e). B, In vitro transfection efficiency of OCMCS/DNA NPs (N/P = 5) and OCMCS-HA/DNA NPs (OCMCS/HA weight ratio = 4) in the absence (gray bars) or presence (hatched bars) of excess of free HA.

### 3.7. Cell transfection in vitro

In the present work, we evaluated the capacity of OD NPs and OHD NPs to transfect Caco-2 cells. For this purpose, we used a green fluorescent protein-encoding plasmid (pEGFP) as a reporter gene. Fig. 5 shows the levels of expressed enhanced green fluorescence protein (EGFP) obtained after incubation of the pEGFP-loaded NPs in the Caco-2 cells. Naked pDNA was placed as a control, and no expression of the protein was detected. The expressed EGFP in Caco-2 cells transfected with OHD NPs was about 5-fold higher than OD NPs, but, it was still about two to three times lower than that of the Lipofectamine<sup>TM</sup> 2000 DNA complex group. The results showed that the ability of the NPs to transfect cells was strongly influenced by their composition. EGFP-positive transfected cells were detected by fluorescence microscopy at 48 h after transfection (Fig. 6A). The fluorescent images of Caco-2 cells transfected with complex NPs also confirmed the FACS analysis above.

This enhancement of the transfection efficiency of OHD NPs could be a result of the presence of HA in the NP composition. First, HA could be expected to improve the internalization of the NPs as a result of specific and nonspecific interactions with the cells. Second, it has been reported that on internalization, HA is included in nonlysosomal vesicular compartments and rapidly accumulated in the perinuclear region and cell nuclei (Tammi et al., 2001). Hence, trafficking could be speculated for the NPs containing HA that undertake intracellular pathways that favor the gene expression. Third, HA has been described as a transcription activator, which is able to enhance the transfection efficiency of HA-coated PEI complexes (Ruponen et al., 2001). Consequently, the same type of mechanism could apply to the OHD NPs.

In order to investigate the potential utilization of CD44 in aiding transportation of pDNA into the cell, excess of free HA was utilized to block the receptor (Issa et al., 2006). Inhibition experiments with 10 times of free HA showed a significantly 3-fold decrease of gene expression for OHD NPs, whereas OD NPs were barely influenced (Fig. 6B). These results showed that entrance of OHD NPs to the

Caco-2 cell was via ligand–receptor endocytosis by attachment of HA to its receptors at the surface of the epithelial cells. OHD NPs nanoparticles showed good transfection efficiency in Caco-2 cells.

## 4. Conclusions

In this study, OHD NPs were successfully prepared as novel, non-viral vectors for gene delivery. The optimum N/P ratio was found to be 5 with the ideal OCMCS/HA weight ratio of 4 which resulted in the smallest nanoparticles. Involving HA in OHD NPs was beneficial for the DNA release as well as cellular uptake. OHD NPs were capable to deliver DNA to small intestine and released the loaded DNA only when they approached intestinal enterocytes. Compared to Lipofectamine<sup>TM</sup> 2000, both OD NPs and OHD NPs did not show any significant cytotoxicity against Caco-2 cells. The transfection efficiency of OHD NPs was 5-fold higher than that of OD NPs under the same conditions. This study suggested that OHD NPs can be a safe and effective carrier for targeted gene delivery to CD44 of GI system.

## Acknowledgements

This work was supported by grants of International S&T Cooperation Program of China (2011DFA31270) and the National Natural Science Foundation of China (Grant No. 81071246).

## References

- Auruffo, A., Stamenkovic, I., Melnick, M., Underhill, C. B., & Seed, B. (1990). CD44 is the principal cell surface receptor for hyaluronate. *Cell*, 61(7), 1303–1313.
- Casu, B., & Gennaro, U. (1975). A conductometric method for the determination of sulphate and carboxyl groups in heparin and other mucopolysaccharides. *Carbohydrate Research*, 39, 168–176.
- Duceppe, N., & Tabrizian, M. (2009). Factors influencing the transfection efficiency of ultra low molecular weight chitosan/hyaluronic acid nanoparticles. *Biomaterials*, 30, 2625–2631.
- Elfinger, M., Geiger, J., Hasenpusch, G., üzgün, S., Sieverling, N., Aneja, M. K., Maucksch, C., & Rudolph, C. (2009). Targeting of the beta(2)-adrenoceptor

- increases nonviral gene delivery to pulmonary epithelial cells in vitro and lungs in vivo. *Journal of Controlled Release*, 135, 234–241.
- Gao, Y., Xu, Z. H., Chen, S. W., Gu, W. W., Chen, L. L., & Li, Y. P. (2008). Arginine-chitosan/DNA self-assemble nanoparticles for gene delivery: In vitro characteristics and transfection efficiency. *International Journal of Pharmaceutics*, 359, 241–246.
- Hu, Y., Jiang, X., Ding, Y., Ge, H., Yuan, Y., & Yang, C. (2002). Synthesis and characterization of chitosan-poly(acrylic acid) nanoparticles. *Biomaterials*, 23, 3193–3201.
- Issa, M. M., Köping-Höggård, M., Tømmeraas, K., Vårum, K. M., Christensen, B. E., Strand, S. P., & Artursson, P. (2006). Targeted gene delivery with trisaccharide substituted chitosan oligomers in vitro and after lung administration in vivo. *Journal of Controlled Release*, 115, 103–112.
- Lai, S. K., Wang, Y. Y., & Hanes, J. (2009). Mucus-penetrating nanoparticles for drug and gene delivery to mucosal tissues. *Advanced Drug Delivery Reviews*, 61, 158–171.
- Li, S. D., & Huang, L. (2006). Targeted delivery of antisense oligodeoxynucleotide and small interference RNA into lung cancer cells. *Molecular Pharmaceutics*, 3(5), 579–588.
- Li, Y. Y., Chen, X. G., Yu, L. M., Wang, S. X., Sun, G. Z., & Zhou, H. Y. (2006). Aggregation of hydrophobically modified chitosan in solution and at the air-water interface. *Journal of Applied Polymer Science*, 102, 1968–1973.
- Liu, Y., Cheng, X. J., Dang, Q. F., Ma, F. K., Chen, X. G., Park, H. J., & Kim, B. K. (2012). Preparation and evaluation of oleoyl-carboxymethyl-chitosan (OCMCS) nanoparticles as oral protein carriers. *Journal of Materials Science: Materials in Medicine*, 23(2), 375–384.
- Liu, Y., Zang, H. D., Kong, M., Ma, F. K., Dang, Q. F., Cheng, X. J., Ji, Q. X., & Chen, X. G. (2012). In vitro evaluation of mucoadhesion and permeation enhancement of polymeric amphiphilic nanoparticles. *Carbohydrate Polymers*, 89, 453–460.
- Luten, J., van Nostrum, C. F., De Smedt, S. C., & Hennink, W. E. (2008). Biodegradable polymers as non-viral carriers for plasmid DNA delivery. *Journal of Controlled Release*, 126, 97–110.
- Mansouria, S., Cuieba, Y., Winnikb, F., Shia, Q., Lavigne, P., Benderdoura, M., Beaumont, E., & Fernandes, J. C. (2006). Characterization of folate-chitosan-DNA nanoparticles for gene therapy. *Biomaterials*, 27, 2060–2065.
- Mao, H., Roy, K., Troung-Le, V., Janes, K. A., Lin, K. Y., Wang, Y., August, J. T., & Leong, K. W. (2001). Chitosan-DNA nanoparticles as gene carriers: Synthesis, characterization and transfection efficiency. *Journal of Controlled Release*, 70, 399–421.
- Mao, S., Sun, W., & Kissel, T. (2010). Chitosan-based formulations for delivery of DNA and siRNA. *Advanced Drug Delivery Reviews*, 62, 12–27.
- Marhaba, R., & Zoller, M. (2004). CD44 in cancer progression: Adhesion, migration and growth regulation. *Journal of Molecular Histology*, 35(3), 211–231.
- Merdan, T., Kopecek, J., & Kissel, T. (2002). Prospects for cationic polymers in gene and oligonucleotide therapy against cancer. *Advanced Drug Delivery Reviews*, 54(5), 715–758.
- Mohammadi, Z., Abolhassani, M., Dorkoosh, F. A., Hosseinkhani, S., Gilani, K., Amini, T., Rouholamini Najafabadi, A., & Rafiee Tehrani, M. (2011). Preparation and evaluation of chitosan-DNA-FAP-B nanoparticles as a novel non-viral vector for gene delivery to the lung epithelial cells. *International Journal of Pharmaceutics*, 409, 307–313.
- Muzzarelli, R. A. A. (2010a). Chitosans: New vectors for gene therapy. In R. Ito, & Y. Matsuo (Eds.), *Handbook of carbohydrate polymers: Development, properties and applications* (pp. 583–604). Hauppauge, NY, USA: Nova Publication.
- Muzzarelli, R. A. A. (2010b). Chitins and chitosans as immunoadjuvants and non-allergenic drug carriers. *Marine Drugs*, 8(2), 292–312.
- Muzzarelli, R. A. A., Greco, F., Busilacchi, A., Sollazzo, V., & Gigante, A. (2012). Chitosan, hyaluronan and chondroitin sulfate in tissue engineering for cartilage regeneration: A review. *Carbohydrate Polymers*, 89, 723–739.
- Nandedkar, T. D. (2009). Nanovaccines: Recent developments in vaccination. *Journal of Biosciences*, 34, 995–1003.
- Romoren, K., Pedersen, S., Smistad, G., Evensen, O., & Thu, B. J. (2003). The influence of formulation variables on in vitro transfection efficiency and pH physicochemical properties of chitosan-based polyplexes. *International Journal of Pharmaceutics*, 261, 115–127.
- Ruponen, M., Rönkkö, S., Honkakoski, P., Pelkonen, J., Tammi, M., & Urtti, A. (2001). Extracellular glycosaminoglycans modify cellular trafficking of lipoplexes and polyplexes. *Journal of Biological Chemistry*, 276(36), 33875–33880.
- Saboktakin, M. R., Tabatabaie, R. M., Maharramov, A., & Ramazanov, M. A. (2011). Synthesis and in vitro evaluation of carboxymethyl starch-chitosan nanoparticles as drug delivery system to the colon. *International Journal of Biological Macromolecules*, 48, 381–385.
- Schatzlein, A. G. (2001). Non-viral vectors in cancer gene therapy: Principles and progress. *Anti-Cancer Drugs*, 12(4), 275–304.
- Schmitz, T., Bravo-Osuna, I., Vauthier, C., Ponchel, G., Loretz, B., & Bernkop-Schnurch, A. (2007). Development and in vitro evaluation of a thimer-based nanoparticulate gene delivery system. *Biomaterials*, 28, 524–531.
- Tammi, R., Rilla, K., Pienimäki, J. P., MacCallum, D. K., Hogg, M., Luukkonen, M., Hascall, V. C., & Tammi, M. (2001). Hyaluronan enters keratinocytes by a novel endocytic route for catabolism. *Journal of Biological Chemistry*, 276(37), 35111–35122.
- Vadolas, J., Williamson, R., & Ioannou, P. A. (2002). Gene therapy for inherited lung disorders: An insight into pulmonary defence. *Pulmonary Pharmacology & Therapeutics*, 15, 61–72.
- Wan, L. Q., Hu, F. Q., & Yuan, H. (2004). Study of the uptake of chitosan oligosaccharide nanoparticles by A549 cells. *Acta Pharmacologica Sinica*, 39, 227–231.
- Zhao, Q. Q., Chen, J. L., Lv, T. F., He, C. X., Tang, G. P., Liang, W. Q., Tabata, Y., & Gao, J. Q. (2009). N/P ratio significantly influences the transfection efficiency and cytotoxicity of a polyethylenimine/chitosan/DNA complex. *Biological & Pharmaceutical Bulletin*, 32, 706–710.